

High Selectivity Microwave Bandpass Filter With A Wide Upper Stopband

Muhammad RIAZ¹, Bal S VIRDEE²

¹Department of Electrical Engineering, Grand Charter College of Engineering and Technology, Lahore, Pakistan,

²School of Computing & Digital Media, London Metropolitan University, London, UK

Received: .201

• Accepted/Published Online: .201

• Final Version: .201

Abstract: This paper describes a highly selective microwave bandpass filters based on microstrip integrated technology. The filter initially proposed consists of electromagnetically coupled C-shaped open-ring resonators whose feedlines are loaded with inductive spiral shaped open-circuited stubs that are strategically located along the feedlines in order to introduce transmission zeros in the filter's stopband response. It is shown that the overall response and selectivity of this filter can be significantly enhanced by interdigitally coupling the resonators with the feedline. The resulting filter exhibits highly sharp roll-off skirts with a passband insertion-loss of 1.4 and return-loss of greater than 15 dB. The out-of-band rejection level of the filter is greater than 15 dB. Simulation results show that the center frequency of this type of filter can be adjusted from 3.3 to 3.8 GHz by carefully modifying the structure's dimensions. The proposed coupling scheme allows to control the filter's 3 dB fractional bandwidth, and results show the fractional bandwidth of the filter can be adjusted between 5.52 to 17.7% with negligible effect on the stopband characteristics. The proposed filter is suitable for applications in high interference environments and cognitive radio systems.

Key words: Microstrip technology, microwave filters, bandpass filters, high selectivity filters, wide out-of-band rejection

1. Introduction

In wireless communication and radar systems, microwave bandpass filters play a pivotal role to prevent interference from neighboring channels by controlling the frequency response of the transmitter and receiver. The next generation of wireless communication systems require filters of high-performance such as high frequency-selectivity, wide stopband rejection, low insertion-loss, and high return-loss. In addition, these filters need to be compact and low cost to fabricate in mass production. High selectivity and wide stopband rejection are important to increase system capacity and suppress unwanted interference from other systems in a congested EM spectrum. Planar filters implemented with printed circuit technology are attractive, as they are easy and economical to fabricate. However, conventional filters designed using distributed components usually suffer from unwanted spurious responses because of their higher-order resonances. The presence of out-of-band spurious responses can degrade system performance.

Researchers have extensively investigated bandpass filters (BPF) to realize wide stopband response using various techniques in [1-5]. For example, open-circuit transmission-line stubs and interdigital capacitors are used to widen the stopband of conventional J-inverter filters [1]. In [2], "wiggly line" structures realized to reject multiple spurious passbands generated in parallel-coupled-line microstrip BPFs. In [3], resonators that have the same fundamental frequency as the spurious responses but different higher-order resonant frequencies are used to suppress spurious responses in the filter's stopband. In [4], a wide-stopband microstrip BPF design uses quarter-wavelength shorted coupled-lines. Stepped-impedance resonators (SIRs) have been used to shift higher-order resonant frequencies to achieve wide stopband bandpass filters. In addition, the harmonic response of SIR can be controlled by manipulating the impedance ratio of the resonator [5].

In this article, the design of a highly selective planar bandpass filter is presented with a wide stopband necessary to suppress unwanted interference over almost three octaves. The first filter proposed uses electromagnetically coupled C-shaped open-ring resonators that is loaded strategically with inductive

open-circuited stubs to inject transmission zeros in order to realize a wide stopband. The filter is shown to exhibit a highly selective passband transmission response. It is also shown that when the C-shaped open-ring resonators of the proposed filter are interdigitally coupled with the feedline the filter's passband insertion-loss and its stopband rejection level are significantly improved.

1. Theoretical analysis of the stub notch filter

A notch filter allows all frequencies to pass through it except those in its stopband. Figure 1 shows the layout of a microstrip notch filter. The filter comprises a 50Ω microstrip transmission-line which is open-circuit at point S. When a signal of wavelength λ transmitted from point A to B, the length of the open-circuit line needs to be $\lambda/4$ to eliminate it. This is because the open-circuit at S will transform into the short-circuit at the point where the open-circuit line joins with AB and consequently the signals passing along AB will be blocked. The impedance Z_{in} at the junction of the open-circuit stub is:

$$Z_{in} = Z_s \left\{ \frac{Z_L + jZ_s \tan \beta l}{Z_s + jZ_L \tan \beta l} \right\} \quad (1)$$

Where β is the phase constant, Z_s is stub impedance, Z_L is the terminating load impedance, and l is the length of the line. Since $Z_L = \infty$, we can ignore Z_s terms, hence

$$Z_{in} = Z_s \left\{ \frac{Z_L + jZ_s \tan \beta l}{Z_s + jZ_L \tan \beta l} \right\} = -jZ_s \cot \beta l \quad (2)$$

so (2) become

$$Z_{in} = -jZ_s \cot \beta l = 0 \quad (3)$$

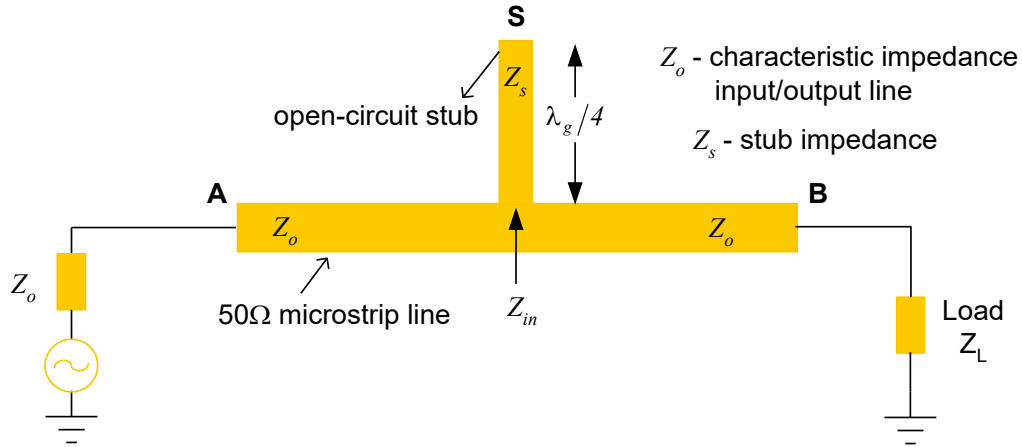


Figure 1. Single stub notch filter.

These results show that a signal with a wavelength of $\lambda_g/4$ will see a very low impedance to ground at point S, which is short-circuited. Hence, the signal with this wavelength will be absorbed from the signals applied at input A, which manifests as high attenuation in its insertion-loss response at its frequency f_o . All other signals remain unaffected, hence low insertion-loss except near f_o . Note, the VSWR is higher at other frequencies since the $\cot \beta l$ term is no longer zero. The expression for the insertion-loss for the above circuit is given below.

$$IL = 10 \log \left[1 + \left(\frac{\bar{Y}_s}{2} \right)^2 \right] \quad (4)$$

$$IL = 10 \log \left[1 + \left(-\frac{Z_o}{2Z_s} \cot \beta l \right)^2 \right] \quad (5)$$

The width of the line determines its impedance, i.e. the higher the impedance the thinner the line and vice versa. When $Z_s = Z_0$, this is equivalent to a width of the stub = width of the input/output transmission-line. So, Equation (5) can be written as

$$IL = 10\log\left[1 + \left(\frac{\cot^2\beta l}{4}\right)\right] \quad (6)$$

So, $IL = 0$ dB at center frequency. When $Z_s > Z_0$, i.e. the width of the stub is less than the input/output transmission-line, the $IL \rightarrow 0$ dB at center frequency.

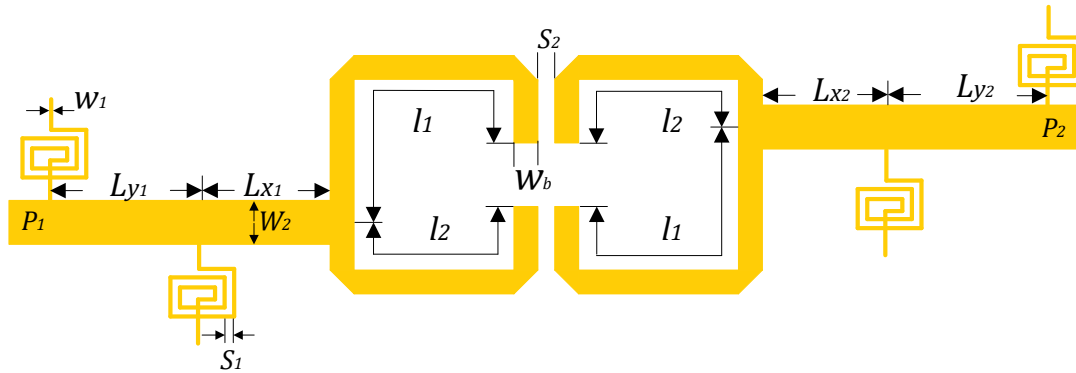
2. Design and analysis of BPF whose feedlines are loaded with open-circuited inductive stubs

The proposed filter structure in Figure 2 comprises two mixed (electric and magnetic) coupled opening resonators where the input and output feedlines are inductively loaded with a pair of open-circuited stubs in the shape of spirals. Spiraled open-circuited stubs keep the filter structure compact. In this configuration strong electromagnetic coupling with the C-shaped open-ring resonator is realized. This filter design is fabricated on standard substrate Arlon CuClad217LX with thickness $h = 0.794$ mm, dielectric constant $\epsilon_r = 2.17$, thickness of conductor $t = 35$ microns, and loss-tangent $\delta = 0.0009$. The characteristic impedance of feedlines is 50Ω with a width of 2.42 mm. The filter was designed at a center frequency of 3.2 GHz and 3 dB bandwidth of 250 MHz. Attenuation zeros are introduced in the filter's transmission response at 2.95 GHz and 3.45 GHz, with corresponding lengths l_1 and l_2 , respectively, calculated using Equations (7) and (8) [6].

$$f_1 = \frac{nc}{4l_1 \sqrt{\epsilon_{eff}}} \quad (7)$$

$$f_2 = \frac{nc}{4l_2 \sqrt{\epsilon_{eff}}} \quad (8)$$

The location of the stubs on the feedlines of the filter were determined through simulation analysis ensuring good in-band performance is maintained. Simulation and optimization were accomplished using Keysight Technologies' Advanced Design System (ADS™) momentum software. The optimized design parameters are: $W_1 = 0.2$ mm, $W_2 = 2.42$ mm, $l_1 = 19.1$ mm, $l_2 = 12.79$ mm, $S_1 = 0.6$ mm, $S_2 = 0.67$ mm, $L_{x1} = 13.37$ mm, $L_{x2} = 29$ mm, $L_{y1} = 21.38$ mm, $L_{y2} = 13.82$ mm, and $W_b = 0.2$ mm. The simulated transmission response of the filter without and with spiral loaded feedlines are shown in Figure 3 (a) & (b). Comparison of these two responses shows that the filter with spiral loading generates three transmission zeros on both sides of the passband response. The transmission zeros at 2.9 GHz and 3.5 GHz correspond to open-stub lengths l_1 and l_2 , respectively, loaded on the feedlines. The spiral loaded feedlines significantly improve the out-of-band rejection performance, which is greater than 15 dB. In addition, the return-loss is better than 16 dB and insertion-loss centered at 3.2 GHz increased to 1.3 dB which mainly attributed to conductor losses. The measured response with spiral loaded feedline, shown in Figure 3 (c), has insertion-loss of 1.7 dB and return-loss better than 15 dB.



(a)

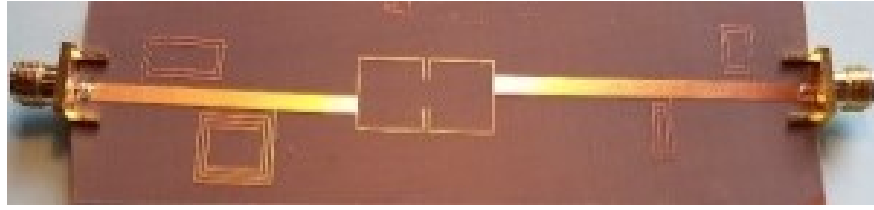


Figure 2. (a) Layout (b) photograph of proposed bandpass filter.

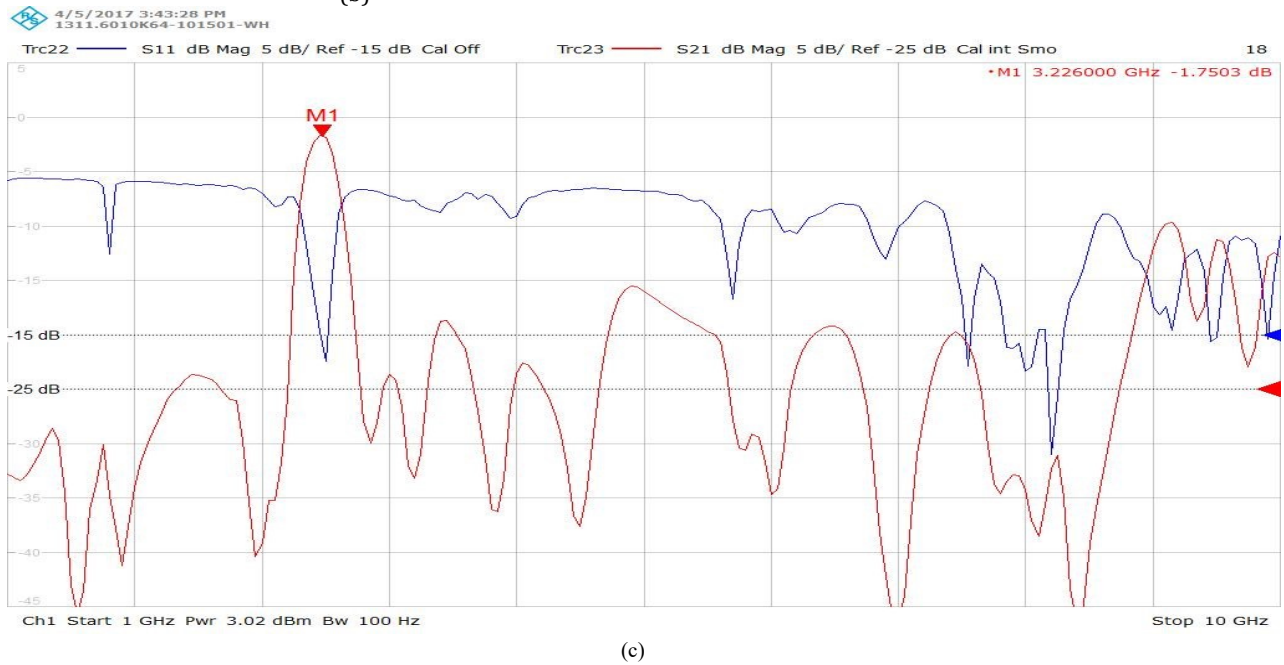
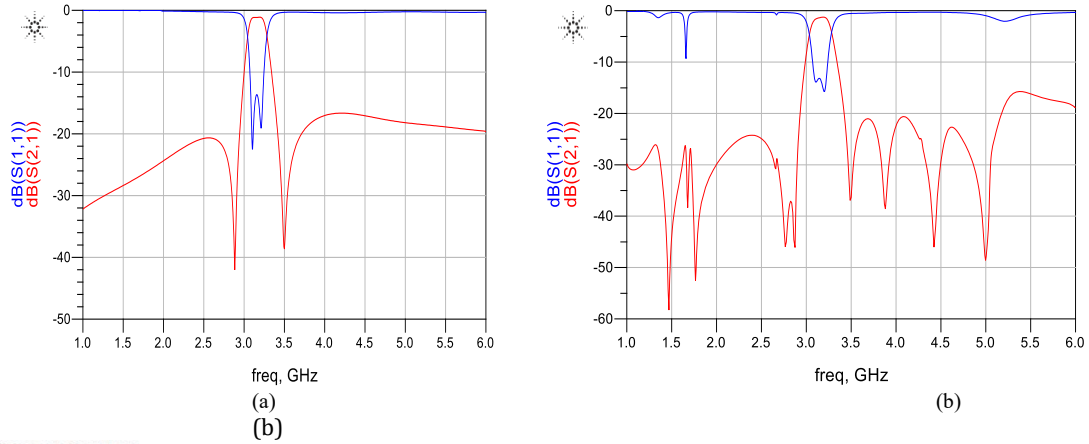


Figure 3. (a) Simulated S-parameter response without spiral loaded feedline (b) Simulated S-parameter response with spiral loaded feedline (c) measured S-parameter response with spiral loaded feedline

3. Interdigitally coupled bandpass filter structure

3.1 BPF configuration and results

The input and output feedline coupling scheme, shown in Figure 2, was modified to that shown in Figure 4, where the C-shaped open-ring resonators are coupled to the input and output via three-finger

interdigital capacitors. The physical dimensions of this filter are: $W_a = 0.2 \text{ mm}$, $l_1 = 2.636 \text{ mm}$, $l_2 = 2 \text{ mm}$, $l_3 = 5.47 \text{ mm}$, $l_4 = 10.69 \text{ mm}$, $L_{b1} = 2 \text{ mm}$, $L_{b2} = 1 \text{ mm}$, $L_{b3} = 15.978 \text{ mm}$, $S_1 = 0.58 \text{ mm}$, $S_2 = 0.277 \text{ mm}$. The simulated and measured responses in Figure 5 show that with this feedline approach the filter response is significantly improved with a flatter passband response with insertion-loss of 1.2 dB and return-loss better than 10 dB, sharper roll-off, steep skirt selectivity and a 3 dB bandwidth of 700 MHz (3.1 to 3.8 GHz) centered at 3.4 GHz with. The filter response exhibits a 3 dB fractional bandwidth of 17.7% and the group-delay in the passband varies between 0.3 to 0.5 ns. In addition, the stopband rejection is >15 dB extending up to 9.4 GHz (i.e. $2.76f_0$). There is excellent correlation between the simulated and measured results.

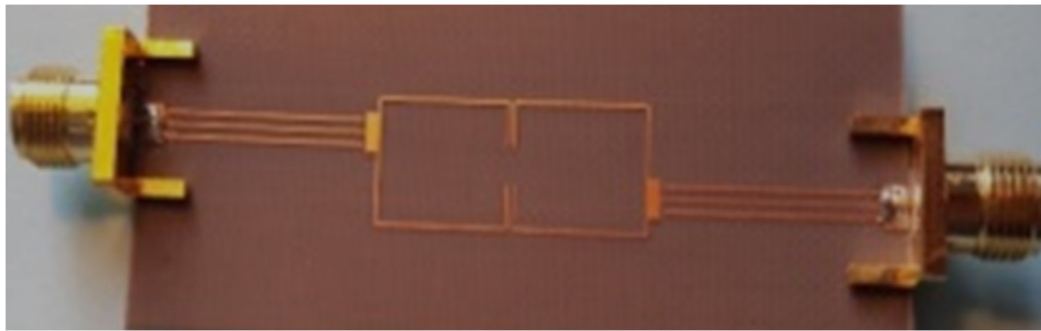
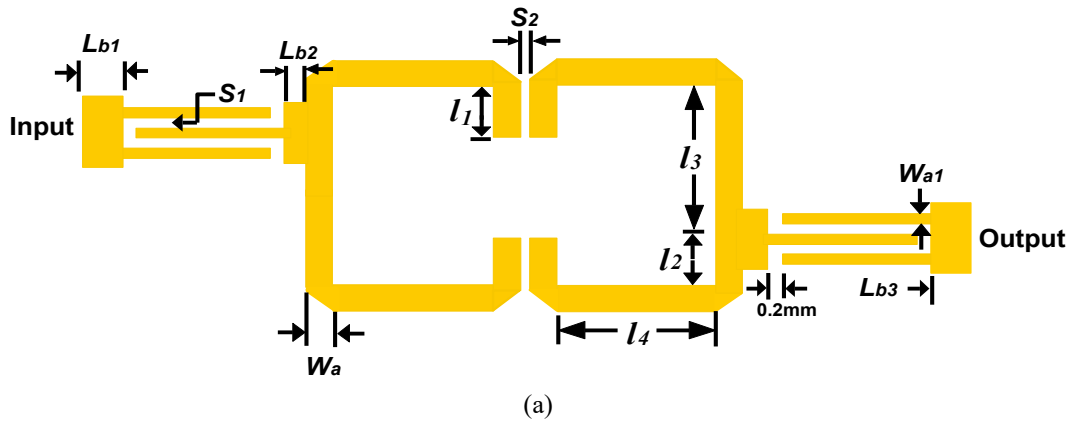
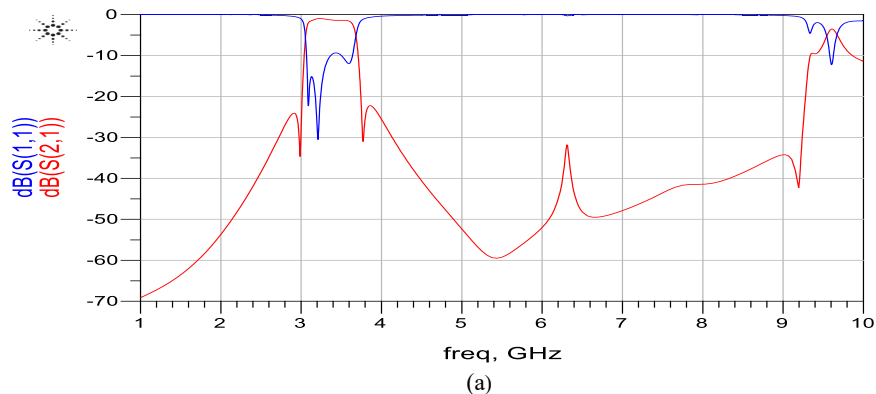
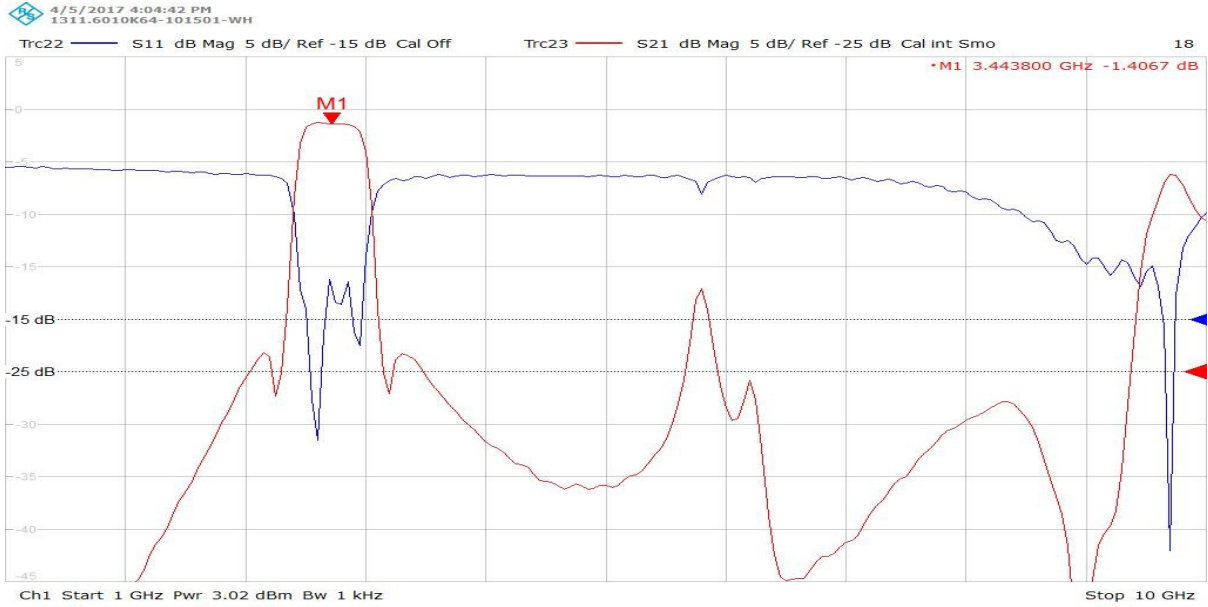


Figure 4. (a) Configuration of the filter with three fingers interdigital coupled feedlines (b) photograph of the proposed filter.

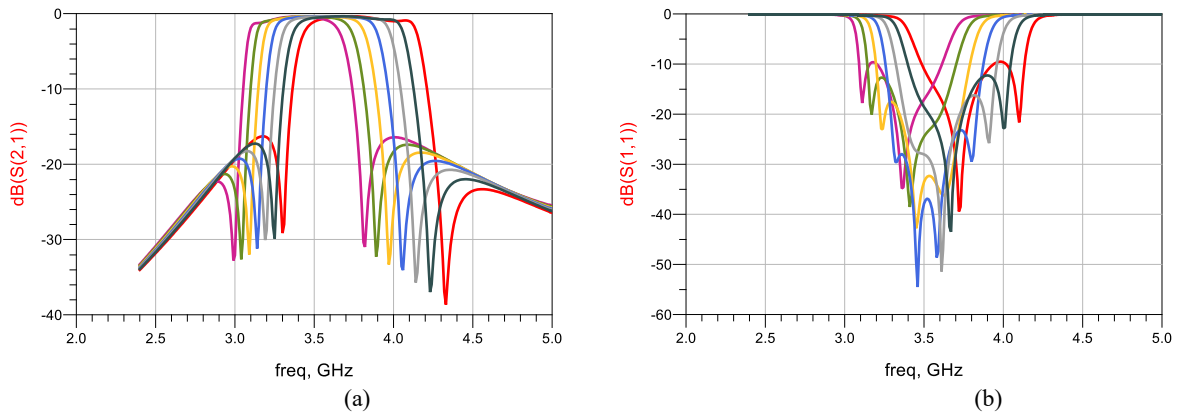




(b)
Figure 5. (a) Simulated S-parameter response of the proposed filter (b) Measured response of the proposed filter

3.2 Adjustable center frequency and transmission zero characteristics

Figure 6 shows that the center frequency of the proposed filter can be changed with negligible effect on the filter's passband shape and overall transmission response. The center frequency shifts by 176 MHz as the resonator length l_4 is varied from 11.09 to 10.29 mm. The tuning range of the center frequency is from 3.3 to 3.8 GHz, and the corresponding insertion-loss varies from 0.53 to 0.98 dB and return-loss from 9.8 to 21 dB. Figure 7 shows that the transmission zeros at the passband upper and lower edges can be controlled independently with insignificant degradation in the frequency response. In fact, the resonator length l_3 controls the lower transmission zero which shifts toward the lower frequencies as the length is changed from 5.47 to 6.07 mm, and the upper transmission zero moves toward the lower frequencies as the resonator length l_2 is changed from 2.2 to 2.8 mm. Small variation in the passband shape is observed with change in lengths l_2 and l_3 .



(a) (b)
Figure 6. Frequency response of the proposed filter as a function of resonator length l_4

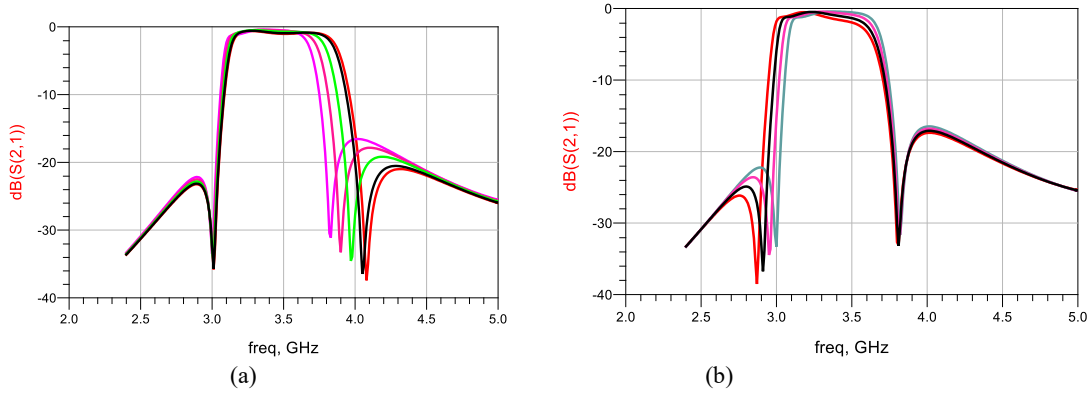


Figure 7. Frequency response of the proposed filter as a function of resonator lengths (a) l_2 (b) l_3

3.3 Fractional bandwidth characteristics

By manipulating the geometric parameters of the interdigital capacitors shown in Figure 4 allows to control the filter's bandwidth. The maximum 3 dB fractional bandwidth achievable is 17.7% with physical dimensions of: $W_a = 0.2$ mm, $l_1 = 2.636$ mm, $l_2 = 2$ mm, $l_3 = 5.47$ mm, $l_4 = 10.69$ mm, $L_{b1} = 2$ mm, $L_{b2} = 1$ mm, $L_{b3} = 15.978$ mm, $S_1 = 0.58$ mm, $S_2 = 0.277$ mm. The minimum 3 dB fractional bandwidth achievable using this configuration is 5.52% and its out-of-band rejection level is ≥ 20 dB across 1 to 3.5 GHz and ≥ 18 dB across 3.3 to 10.4 GHz, as shown in Figure 8. The optimized physical dimensions of the narrow band bandpass filter are: $W_a = 0.2$ mm, $l_1 = 2.536$ mm, $l_2 = 2.736$ mm, $l_3 = 4.136$ mm, $l_4 = 10.47$ mm, $L_{b1} = 2.3$ mm, $L_{b2} = 1.74$ mm, $L_{b3} = 15.3088$ mm, $S_1 = 0.884$ mm, $S_2 = 0.89$ mm.

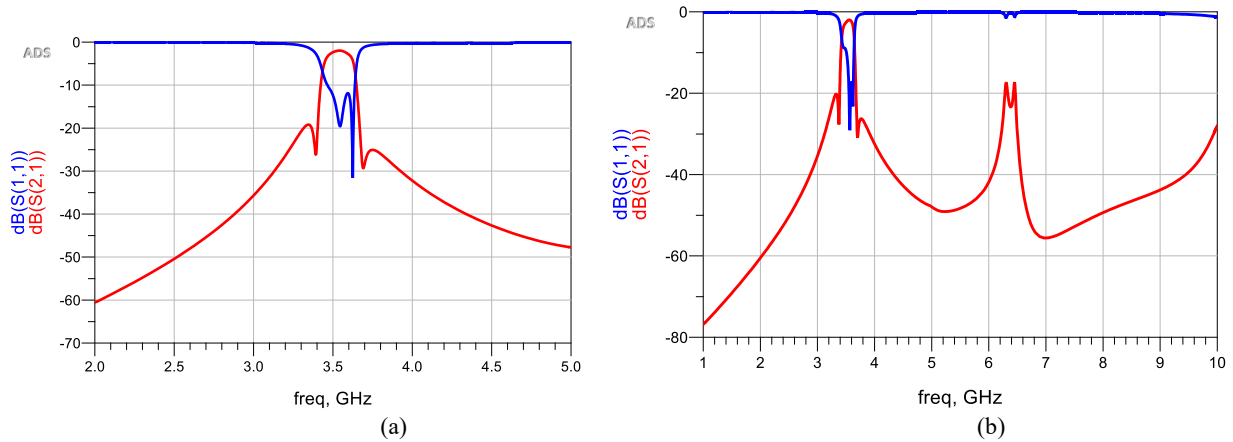


Figure 8. The insertion and return-loss response for the narrow 3-dB fractional bandwidth, (a) Close up view (b) Full response

Table shows the comparison of salient features between the proposed filter and bandpass filters reported in the literature. The proposed filter shows low insertion-loss, high selectivity across its entire tuning range. The proposed filter is of a compact structure that was constructed on a relatively low dielectric substrate and exhibits significantly high out-of-band rejection level over a wide frequency span. Other filter structures reported in the table are of a complex design with a larger footprint and increased fabrication cost.

Table: Comparison of proposed BPF with other published BPFs

	Center frequency (GHz)	Upper stopband (GHz) for $S_{21} \geq 15$ dB	Insertion-loss (dB)	ϵ_r
[9]	1.7–2.7	4	4.9–3.8	2.2
[12]	0.95–1.49	4	4.1–1.6	6.15
[13]	0.77–1.42	2.4	3.1–1.0	3.38
[14]	0.97–1.53	3	4.2–2.0	3.55
[15]	0.95–1.35	2.1	5.6–4.7	3.5
This work	3.3–3.8	9.4	1.2–0.53	2.17

4. Conclusion

The proposed planar microwave bandpass filter is shown to exhibit desirable characteristics of relative low insertion-loss, high return-loss, sharp roll-off skirts, high selectivity and a wide stopband with a high rejection level. The proposed filter is composed of two mixed (electric and magnetic) coupled C-shaped opening resonators that are interdigitally coupled with the feedlines. It is shown that the physical dimensions of the proposed filter configuration can be adjusted to provide a filter with 3 dB fractional bandwidth from 5.5 to 17.7%. These features make the filter applicable in wireless communication systems that operate in highly interfering environments and cognitive radio systems.

References

- [1] C.-W. Tang and Y.-K. Hsu. A microstrip bandpass filter with ultrawide stopband. *IEEE Trans. Microwave Theory Tech* 2008; 56 (6): 1468–1472. doi: 10.1109/tmmt.2008.923900
- [2] T. Lopetegi, M. A. G. Laso, F. Falcone, F. Martin, J. Bonache. Microstrip wiggly-line bandpass filters with multi spurious rejection. *IEEE Microwave Wireless Component Letter* 2004; 14 (11): 531–533. doi: 10.1109/lmwc.2004.837062
- [3] C.-F. Chen, T.-Y. Huang, R.-B. Wu. Design of microstrip bandpass filters with multi order spurious-mode suppression. *IEEE Trans. Microwave Theory Tech* 2005; 53 (12): 3788–3793. doi: 10.1109/tmmt.2005.859869
- [4] X. Luo, H. Qian, J.-G. Ma, K. S. Yeo. A compact wide stopband microstrip bandpass filter using quarter-wavelength shorted coupled lines. *Proc. Asia-Pacific Microwave Conference* 2010; 1142–1145.
- [5] C.H. Kim, K. Chang. Wide-stopband bandpass filters using asymmetric stepped-impedance resonators. *IEEE Microwave Wireless Component Letter* 2013; 23 (2): 69–71. doi: 10.1109/lmwc.2012.2236885
- [6] L. H. Hsieh, K. Chang. Simple analysis of the frequency modes for microstrip ring resonators of any general shape and the correction of an error in literature. *Microwave Optical Technology Letter* 2003; 38 (3): 209–213. doi 10.1002/mop.11017
- [7] B. E. Carey-Smith, P. A. Warr. Broad band-configurable band stop filter design employing a composite tuning mechanism. *IET Microwave Antenna Propagation* 2007; 1 (2): 420–426.
- [8] B. E. Carey-Smith, P. A. Warr. Broad band configurable band stop filter with composite tuning mechanism. *Electron. Letter* 2004; 40 (25): 1587–1589.
- [9] Pei-Ling Chi, Tao Yang, Tsung-Ying Tsai. A Fully Tunable Two-Pole Bandpass Filter. *IEEE Microwave and Wireless Components Letters* 2015; 25 (5): 292 – 294. doi: 10.1109/lmwc.2015.2409794
- [10] Y.- H. Chun, J.-S. Hong. Electronically reconfigurable dual-mode microstrip open-loop resonator filter. *IEEE Microwave Wireless Component Letter* 2008; 18 (7): 449–451. doi: 10.1109/lmwc.2008.924922
- [11] W. Tang, J.-S. Hong. Varactor-tuned dual-mode bandpass filters. *IEEE Transaction Microwave Theory and Techniques* 2010; 58 (8): 2213–2219. doi: 10.1109/lmwc.2018.2870934

- [12] Xiu Yin Zhang, Quan Xue. High-Selectivity tunable bandpass filters with harmonic suppression. *IEEE Transaction Microwave Theory and Techniques* 2010; 58 (4): 964 – 969. doi: 10.1109/tmtt.2010.2042844
- [13] Jian-Xin Chen, Yalin Ma, Jing Cai. Novel Frequency-Agile bandpass filter with wide tuning range and spurious suppression. *IEEE Transaction on industrial electronics* 2015; 62 (10): 6428 – 6435. doi: 10.1109/tie.2015.2427122
- [14] Li Gao, Gabriel M. Rebeiz. A 0.97–1.53-GHz Tunable Four-Pole Bandpass Filter With Four Transmission Zeroes. *IEEE Microwave and Wireless Components Letters* 2019. 29 (3): 195 – 197. doi: 10.1109/lmwc.2019.2895558
- [15] Kaijun Song, Weijia Chen, Shema Richard Patience, Yuxuan Chen, Abdel qani Mohamed Iman. Compact Wide-Frequency Tunable Filter With Switchable Bandpass and Bandstop Frequency Response. *IEEE Access* 2019; 7: 47503 – 47508. doi: 10.1109/access.2019.2908453